MATERIALS CHARACTERIZATION 60 (2009) 775–782

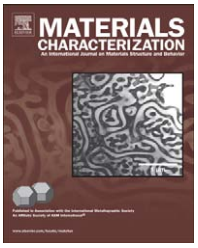

Use of digital speckle pattern correlation for strain measurements in a CuAlBe shape memory alloy

F.M. Sánchez-Arévalo[a,*], T. García-Fernández[b], G. Pulos[c], M. Villagrán-Muniz[a]

[a]Centro de Ciencias Aplicadas y Desarrollo Tecnológico-CCADET, Universidad Nacional Autónoma de México, Cd. Universitaria A.P. 70-186, México D.F. C.P. 04510, México

[b]Universidad Autónoma de la Ciudad de México (UACM), Prolongación San Isidro 151, Col. San Lorenzo Tezonco, México D.F., C.P. 09790, México

[c]Instituto de Investigaciones en Materiales, Universidad Nacional Autónoma de México, Cd. Universitaria A.P. 70-360, México, D. F. C.P. 04510, México

ARTICLE DATA

Article history:
Received 23 September 2008
Received in revised form
6 January 2009
Accepted 14 January 2009

Keywords:
Strain measurements
Speckle pattern
Digital image correlation
Shape memory alloy
CuAlBe
Mechanical behavior

ABSTRACT

A Cu–Al 11.2 wt.%-Be 0.6 wt.% shape memory alloy was subjected to a uniaxial tension test using an MTS load frame with an attached optical microscope. Digital images of the sample's surface were acquired using white light and He–Ne laser illumination. The obtained images were associated to the engineering stress–strain behavior, which was calculated from the measured displacement, strain and force. From the images, displacement vector fields were calculated for white light and laser illumination by digital image correlation (DIC) and digital speckle pattern correlation (DSPC) techniques respectively. Using white light it was possible to observe the grains and the martensitic phase transformation of the material more clearly than using DSPC; nevertheless, better quantitative results of displacement, in-plane strain and elastic moduli were obtained using DSPC than using DIC when they were compared to the reference values measured by electrical extensometry. Furthermore DIC and DSPC work as complementary techniques to determined the micro and macromechanical behavior of the CuAlBe shape memory alloy.

1. Introduction

The combination of techniques developed in different branches of science has been used to measure physical phenomena with more accuracy. This interaction has produced powerful tools to study the materials behavior at different scales. Particularly, the digital image correlation (DIC) and the speckle metrology have provided, separately, two methodologies to characterize the mechanical behavior of materials [1–7].

The combination of these techniques has produced the digital speckle pattern interferometry (DSPCI) and the digital speckle pattern correlation (DSPC) techniques. The DSPCI is a powerful technique that it is capable to measure in-plane strains but complex optical systems are needed [8–10] while DSCP is a technique used to measure in-plane displacements easily from which strains can be calculated [11–13]. This technique is based on the comparison of the speckle patterns formed on the surface of the sample.

When a stress is applied to a sample a strain is produced. This strain induces a surface change provoking a change in the speckle pattern. Hence the speckle pattern is like a "finger print" which represents a particular strain state of the material; if the state of strain changes the speckle pattern changes, changes in the strain state can be determined by tracking the changes in the speckle pattern.

The digital image correlation and speckle metrology techniques represent a helpful alternative to determine strain fields. In previous works different algorithms have been reported to estimate the optical flow–relative change of position–between frames in two different configurations [1,3,14,15]. To improve the correlation between two images,

* *Corresponding author*. Tel.: +52 55 5622 4602; fax: +52 55 5622 4602.
E-mail address: fsanchez@iim.unam.mx (F.M. Sánchez-Arévalo).

1044-5803/$ – see front matter © 2009 Elsevier Inc. All rights reserved.
doi:10.1016/j.matchar.2009.01.006

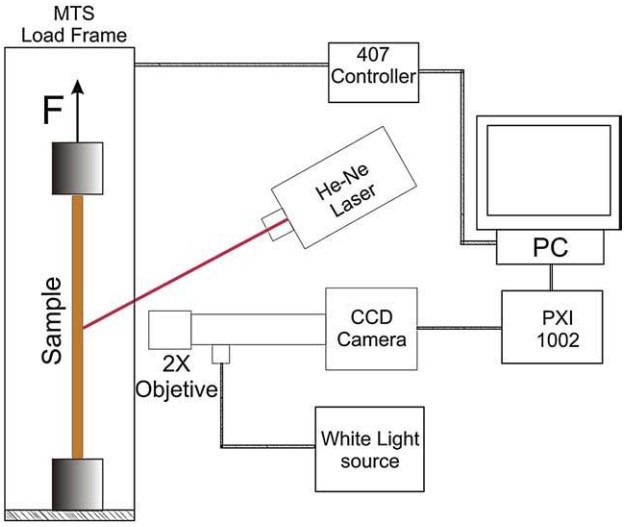

Fig. 1 – Experimental set up.

different methods have been used to get a high contrast random pattern on the surface of the sample including painting, marking or chemically modifying it [16–19]. The speckle pattern is a non-contact alternative that places the high contrast random pattern on the surface of the sample without modifying it. That is why some authors have been using it to observe the mechanical response of conventional materials [20–22].

Although there are different studies which have previously reported the mechanical behavior of materials using DSPC most of them have only a qualitative character. At the same time the stress-induced martensitic transformation has not been studied using the DSPC technique until now. The objective of this work is to study the stress-induced martensitic transformation, under uniaxial tensile test in a 2D-confined[1] CuAlBe polycrystalline shape memory alloy, by DSCP, DIC and electrical extensometry techniques.

2. Experimental Details

Tensile tests have been carried out on a servohydraulic loading device (MTS 858 MiniBionix axial). To acquire images an optical microscope was coupled to a CCD camera (640×480 pixels) as shown in Fig. 1. The modular microscope works as an infinity-corrected compound microscope with magnifications of 2×. To control the MiniBionix MTS a 407 MTS controller was used while data and images were acquired using a National Instruments PXI-1002 chassis and PXI-boards (6281, 8331 and 1402) connected to a PC.

2.1. *Sample Preparation and Illumination Systems*

A Cu–Al 11.2 wt.%–Be 0.6 wt.% shape memory alloy (CuAlBe) was obtained by a melting process and then the ingot was hot-rolled to obtain thin sheets [24]. The sheets were machined in a CNC machine and tensile specimens were obtained having a width of 3 mm, thickness of 0.68 mm and an equivalent length[2] of 25.88 mm. The surface of the sample was mechanically polished and chemically etched with ferric chloride to reveal the grains of the material. Two optical textures (gray-scale distributions on the image) were obtained using white light illumination (150 W quartz halogen light source) and He–Ne laser light (Metrologic Neon laser 632 nm 20 mW). With the white light the metallographic texture can be observed while the speckle pattern appears when the He–Ne laser is used. The sequences of the images, with different optical textures, were analyzed to calculate displacement vector fields using the Willert and Gharib algorithm [15].

2.2. *System Calibration*

Before the microscope was used for strain measurements, it was calibrated using both white light and He–Ne illuminations. By comparing images where there was no rigid body motion or strain, the null field can be determined; the (apparent) displacement vector field in this case is due to vibration and changes in illumination. From these calculations, an error in displacement or optical noise can be calculated. The error–in pixels–can be expressed in microns by calculating the pixel size, which was determined from acquired images of a calibration slide using white light.

Translation experiments were carried out to determine the maximum detectable displacements for both types of illumination. The translations were applied using the servohydraulic control of the MTS load frame; the resulting displacements of the DIC calculations were also compared against a Mitutoyo Digital Indicator. With these procedures, the minimum and maximum detectable displacements were established.

2.3. *Strain Measurements*

With the series of images acquired during the tension test, displacement vector fields were calculated from pairs of images for each illumination type. The Willert and Gharib algorithm [15] was used to calculate $u_k(x_k, y_k)$ and $v_k(x_k, y_k)$, where u and v represent the displacement of an analysis object in the x and y directions respectively [25,26]. The x and y represent the position coordinates of the analysis object in every image; subindex k indicates the corresponding object, which is defined as a 64×64 pixels area. The in-plane strains were determined by minimizing the errors of a six parameters linear model (typically used in linear elasticity theory) given by:

$$u_k(x_k, y_k) = A_1 x_k + B_1 y_k + C_1 + \delta_u(x_k, y_k) \quad (1a)$$

$$v_k(x_k, y_k) = A_2 x_k + B_2 y_k + C_2 + \delta_v(x_k, y_k) \quad (1b)$$

The minimization returns values for the A's, B's and C's where $A_1 = \varepsilon_x$ (strain in x direction), C_1 = translation in x

[1] Refers to a configuration where the thickness of the sample is the same as the grain size (a single quasi-2D layer of coarse grains) [23].

[2] Length of a rectangular strip with the same width and thickness that would exhibit the same force-displacement behavior as the tensile specimen [25].

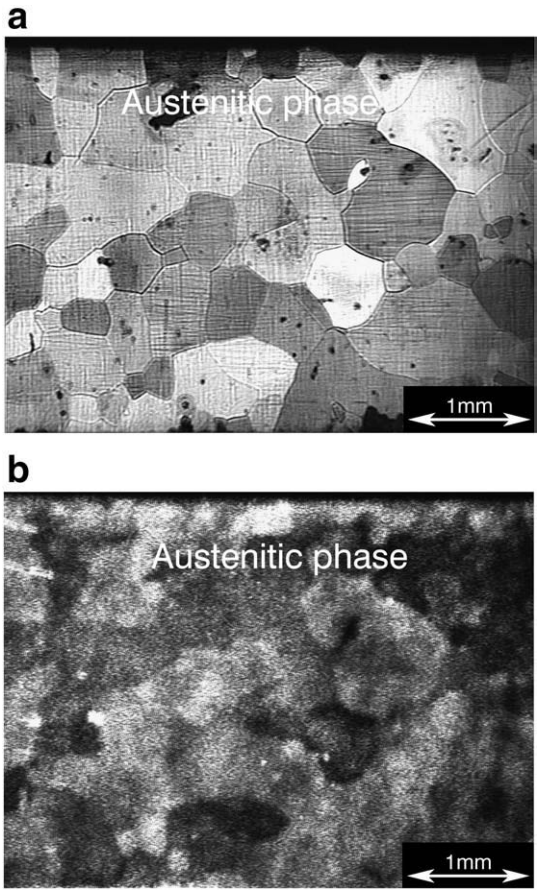

Fig. 2 – Optical textures of the sample obtained using a) white light and b) He–Ne laser without strain neither rigid body motion.

direction, $B_2=\varepsilon_y$(strain in y direction) and C_2=translation in y direction. B_1 and A_2 are linear combinations of shear strain and rotation where the shear strain $\varepsilon_{xy}=(A_2+B_1)/2$ and the rotation $\theta=(A_2-B_1)/2$; $\delta_u(x_k, y_k)$ and $\delta_v(x_k, y_k)$ represent the (small) errors to be minimized.

The minimization functions[3], for each direction, are given by χ^2 expressed in Eqs. (2a) and (2b), where n is the number of analysis objects representing the entire displacement vector field between two images.

$$\chi_u^2 = \sum_{k=1}^{n} [u_k - (A_1x_k + B_1y_k + C_1)]^2 \quad (2a)$$

$$\chi_v^2 = \sum_{k=1}^{n} [v_k - (A_2x_k + B_2y_k + C_2)]^2 \quad (2b)$$

Finding a local minimum in these equations, the in-plane strains were calculated for DIC and DSPC. In order to have another measurement of strain for comparison purposes, an electrical strain gage was bonded on the same region of interest; thus, the macro and micromechanical behavior of the material were determined at the same time.

[3] In this case, the Euclidean norm of the errors $\delta_u$andδ_v is used.

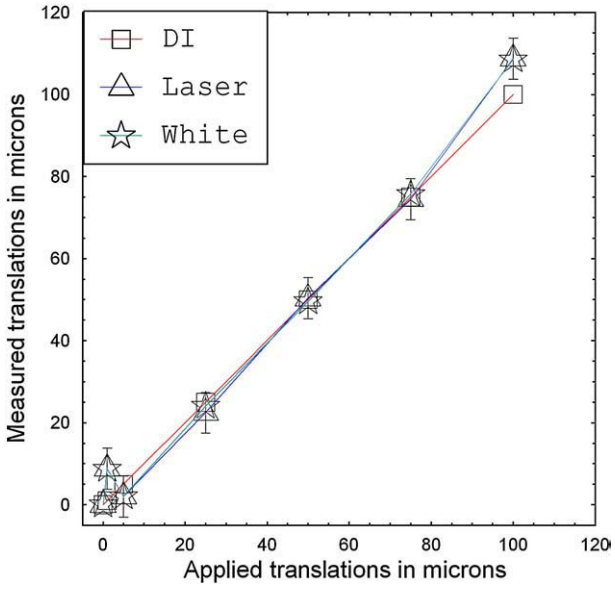

Fig. 3 – Minimum and maximum detectable displacements on pure translation.

3. Results

In Fig. 2 the optical textures for both illumination types are presented. Fig. 2a shows a typical metallographic image of the CuAlBe sample where grains can be observed using white light. These images were taken without any rigid body motion or straining. In Fig. 2b, the speckle pattern that was diffracted on the same region using a He–Ne laser can be observed. In this case the grain boundaries are not clearly observed but the spatial frequencies–a measure of how fast the contrast changes/unit distance–are higher and thus better for the correlation procedure than the spatial frequencies obtained using white light.

To calibrate the system for each illumination type, the noise, the pixel size and the minimum and maximum detectable displacements were determined. The noise,

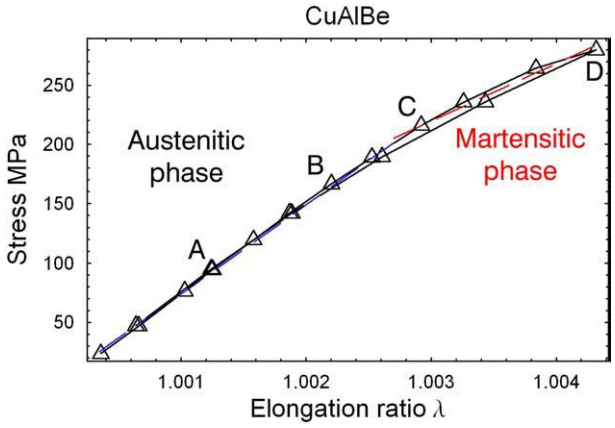

Fig. 4 – Macromechanical behavior: Stress–Strain Curve.

without any rigid body motion or strain, was calculated by acquiring ten images and calculating the mean x and y translations using Eqs. (2a) and (2b). In this case the noise, due to vibration or illumination changes, was 4 to 6% smaller using He–Ne laser illumination than using white light. The speckle pattern works as fine–small–tracers on the surface of the sample resulting in higher spatial frequencies and a better correlation between frames. In addition the pixel size was determined using an Edmund Optics' calibration slide, which in this case turned out to be 6.8 μm in the object space.

During the translation experiments, the minimum and maximum detectable displacements were calculated to establish the displacement range that was employed during the tension test. Fig. 3 shows the displacement range, in microns, where translation measurements were in good agreement using the correlation algorithm for both illumination types. These measurements were compared against the digital indicator (DI) that is considered as the reference measurement of displacement. The best accuracy (±5 μm) was obtained for an increment in displacement between 20 and 80 μm; the

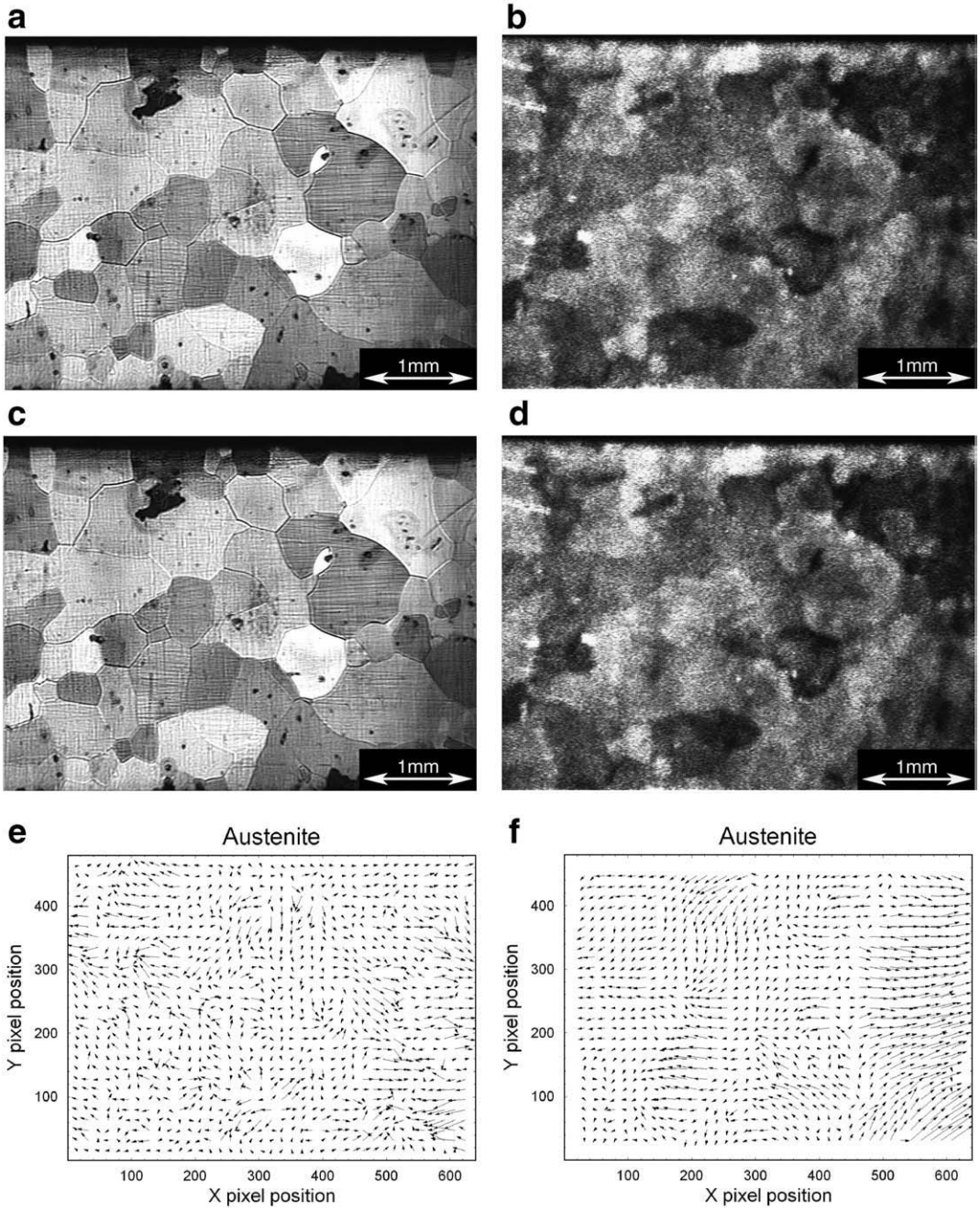

Fig. 5 – Images of the surface's sample associated to the points A and B in Fig. 4. a) Corresponding to point A with white light illumination, b) Corresponding to point A with laser illumination, c) Corresponding to point B with white light illumination and d) corresponding to point B with laser illumination, e) Displacement vector fields at austenitic phase obtained from images 5a and 5c, f) Displacement vector fields at martensitic phase from images 5b and 5d.

acquired images during the tensile experiment were taken within the range of detectable limits.

From the tensile test the stress–strain curve was obtained and it is shown in Fig. 4. The stress–strain curve corresponds to the macromechanical behavior–obtained with the strain gage–of the polycrystalline shape memory alloy. In this case a non-linear behavior is observed and a small superelastic loop too. The first region (A to B of the curve) belongs to the austenitic phase and the second one (C to D) corresponds to a mixture of austenitic phase with martensite plates.

The modulus–slope–of each region was obtained from a least square analysis. The Austenitic region has a modulus around 75±2 GPa while the phase where martensite plates have appeared has a modulus around 49±2 GPa. This change in modulus is due to the stress-induced martensitic transformation, which depends on the applied force, its direction and the crystallographic orientation of grains [27]. It is clear that the strain gage is capable of detecting the martensitic transformation since the detected change in modulus is associated to the additional "transformational" strain that appears when the plates are forming.

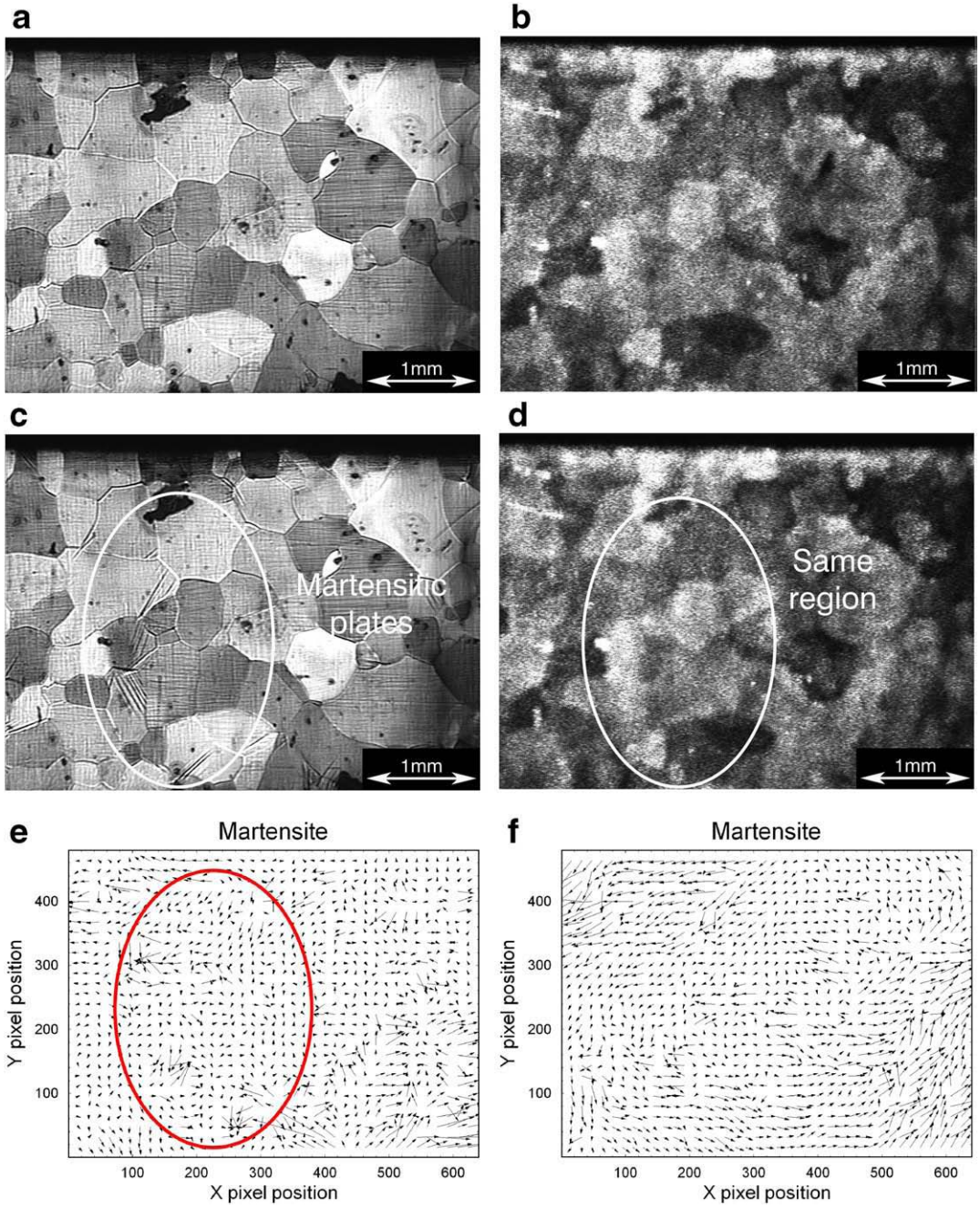

Fig. 6 – Images of the surface's sample associated to the points C and D in Fig. 4. a) corresponding to point C with white light illumination, b) corresponding to point C with laser illumination, c) corresponding to point D with white light illumination and d) corresponding to point D with laser illumination, e) Displacement vector fields at austenitic phase obtained from images 6a and 6c, f) Displacement vector fields at martensitic phase from images 6b and 6d.

Table 1 – Strain measurements.

Phase	Strain using white light [με]	Strain using laser light [με]	Strain gage [με]
Austenitic region A to B	410±20	1090±30	950±15
Martensitic region C to D	580±40	1290±50	967±15

Fig. 5 shows the sample's surface images and the displacement vector fields corresponding to the austenitic phase. Fig. 5a and c show the surface of the CuAlBe sample using white light while Fig. 5b and d show the same region with He–Ne laser illumination. The increments in stress and strain, between point A and B, were 72 MPa and 950 με respectively.

The resulting displacement vector fields, from point A to B, are shown in Fig. 5e and f. Fig. 5e shows the vector field using the DIC while Fig. 5f shows the vector field using DSPC. This last displacement vector field shows the expected hyperbolic field from a uniaxial tension test. In contrast, the displacement vector field obtained by DIC shows a distorted hyperbolic field. Furthermore, the spots of the speckle pattern, used as non-contact fine tracers, improve the correlation process. This process depends on the size of the object of analysis, the displacement between frames and the gray scale distribution on the image [15]. If the size of the image is small (640×480 pixels) a high spatial frequency is needed because the objects of analysis have to be small (64×64 pixels or less). But if the image size is big (3000×4000 pixels), the objects of analysis can be as big as 256×256 pixels and a high spatial frequency is desirable but not necessary [5].

Fig. 6 shows the sample's surface images and the displacement vector fields corresponding to the mixture of martensitic and austenitic phases. When the stress is increased the martensite plates appear in some grains as shown in Fig. 6c. This effect is more clearly observed using white light than using laser illumination (see Fig. 6c and d). The increments in stress and strain, between point C and D, were 52 MPa and 960 με respectively.

The images 6a–c and b–d were used to calculate the displacement vector fields. Fig. 6e shows a region where martensitic plates appeared. In this region the displacement vectors change their directions and magnitudes; this change is more easily observed using white light (Fig. 6c) than using laser illumination (Fig. 6d). In the case where the image is illuminated by white light, the appearance of the martensitic plates changes the contrast locally in the image—since one is able to observe the dark lines representing the martensite plates. Thus one is no longer comparing two images without a change in contrast or light intensity, which is one of the assumptions in the displacement field calculation. Hence, the calculated vectors may represent noise instead of the associated displacement that comes from the transformational strain.

In the case of laser illumination, the speckle pattern does not seem to be affected by the martensite plates and that results in a displacement vector field that is smoother[4]. It seems that these calculations cannot detect the local (transformational) strain associated with each martensite plate; however, a shear strain–perhaps coupled to a rotation–appears, as can be seen from the upper left and lower right corners in Fig. 6f. This shear strain is due to the stress-induced martensitic transformation as was reported in literature [28–30]. In this case (Fig. 6e and f) the displacement vector field is more accurately calculated using laser than using white light; likewise in the case of the austenitic phase (Fig. 5e and f).

From Eq. (2a) the strain associated with the loading direction ($\varepsilon_x = A_1$) was calculated for each illumination type and was also compared with the strain measured with the electrical strain gage. The results are summarized in Table 1.

From Table 1 it is possible to observe that the strain calculated from the images illuminated with white light was almost half of the strain measured with the strain gage. At this point it is obvious that the combination of a small resolution camera and an image with low spatial frequencies is not adequate to measure the strain in this case. Nevertheless, a small camera can be used with white light illumination if the resulting image of the surface of the material presents a random pattern of light intensity–with high spatial frequencies–[16,18].

From the strain measurements and the stress increments the elastic modulus was calculated for the austenitic phase and for the mixture of phases. The results, presented in Table 2, show that DSPC offers a better alternative to measure strain in a CuAlBe sample.

Finally, one would be tempted to draw some conclusions from the displacement vector field and the associated microstructure. While there seems to be a relationship between a single grain and its displacement vectors, several issues must be resolved before a discussion is made. Two of the main hurdles seem to be the change in light intensity associated with the appearance of the martensite plates and the resolution of the measurements (pixel size, image size and number of vectors/grain). The DIC procedure assumes that the light intensity remains constant while the image is deformed, which is clearly not the case–at least with white light–when the phase change takes place.

The issue of resolution can be improved with the use of digital SLR cameras and pixel and image size can be changed with optics; however, one still needs a large enough number of grains to "capture" the macroscopic behavior while having enough resolution to measure the transformational strain. With the current set-up–a CCD camera with a resolution of

Table 2 – The elastic modulus of Cu–Al–Be.

Phase	Micromechanical behavior		Macromechanical behavior
	Elastic moduli [GPa]		Elastic moduli [GPa]
	White light	Laser	σ–ε curve
Austenitic region A to B	178±9	67±2	75±2
Martensitic region C to D	62±6	40±2	49±2

[4] It is for this reason that the oval is not shown in Fig. 6f.

640×480 pixels–,one can only detect some of the effects of the phase change, such as the induced shear strain.

4. Conclusion

In this work three different techniques–digital image correlation, digital speckle pattern correlation and electrical extensometry–have been used to determined the macro and micromechanical behavior of a shape memory alloy.

The DSPC has been successfully exploited to measure the displacement vector field during a uniaxial tension test in a 2D-confined CuAlBe shape memory alloy with a better accuracy than DIC. The speckle pattern establishes a non-contact alternative to get the random illumination patterns on the sample surface. The small non-contact tracers improve the correlation process so low resolution cameras (640×480 pixels) can be used to measure displacements when the surface of the material does not have high spatial frequencies. Better quantitative result of displacement, in-plane strain and elastic moduli were obtained by DSPC when they were compared to the reference measurements (strain gage).

DSPC yields better quantitative results than DIC; nevertheless DIC offers better visual information than DSCP. Thus, both techniques can complement each other.

Acknowledgments

This work was developed with financial support from the PAPIIT DGAPA-UNAM program through grants IN100706, IX121504 and from CONACyT through grants P47758212 and NC204. UNAM CTIC-DGAPA provided a postdoctoral fellowship for F.M.S.A. and additional resources were provided by the ICyTDF program (Instituto de Ciencia y Tecnologia del Distrito Federal).

The authors are grateful to Luis A. Ferrer and Mario Acosta for the use of the electrical strain gage equipment, to Gabriel Lara for his technical support, to Roberto Zenit and Juan Hernández-Cordero for their comments.

REFERENCES

[1] Sutton MA, Cheng M, Peters WH, Chao YJ, McNeill SR. Application of optimized digital correlation method to planar deformation analysis. Image Vis Comput 1986;4:143–50.
[2] Chevalier L, Calloch S, Hild F, Marco Y. Digital image correlation used to analyze the multiaxial behavior of rubber-like materials. Eur J Mech A/Solids 2001;20:169–87.
[3] Hild F. Correli: a software for displacement field measurements by digital image correlation. Internal report no. 254. Universidad de Paris; 2002.
[4] Watrisse B, Chrysochoos A, Muracciole JM, Némoz Guillard M. Analysis of strain localization during tensile test by digital image correlation. Eur J Mech A/Solids 2000;20:189–211.
[5] Sánchez-Arévalo FM, Pulos G. Use of digital image correlation to determine the mechanical behavior of materials. Mater Charact 2008;56:1572–9.
[6] Asakura T. Surface roughness measurement. In: Erf RK, editor. Speckle Metrology. Orlando, FL: Academic Press; 1978.
[7] Yamaguchi I. Speckle displacement and decorrelation in the diffraction and image fields for small object deformation. Opt Acta 1981;28:1359–76.
[8] Wei A, Torgny EC. Speckle interferometry for measurement of continuous deformations. Opt Lasers Eng 2004;40:529–41.
[9] Kumar Rajesh , Singh IP , Shakher Chandra. "Measurement of out-of-plane static and dynamic deformations by processing digital speckle pattern interferometry fringes using wavelet transform". Optics and Lasers in Engineering. Vol. 41. pp. 81–93; 2004.
[10] Li Xide, Wang Kai, Deng Bing. Matched correlation sequence analysis in temporal speckle pattern interferometry. Opt Laser Technol 2004;36:315–22.
[11] Johnson P. Strain field measurements with dual-beam digital speckle photography. Opt Lasers Eng 1998;30:315–26.
[12] Silvennoinen R, Hyvärinen V, Raatikainen P, Peiponen KE. Dynamic laser speckle pattern in monitoring of local deformation of tablet surface alter compression. Int J Pharm 2000;199:205–8.
[13] Jin Guangchang, Wu Zhen, Bao Nikeng, Yao Xuefeng. Digital speckle correlation method with compensation technique for strain field measurements. Opt Lasers Eng 2003;39:457–64.
[14] Barron JL, Flett DJ, Beauchemin SS, Burkitt TA. Performance of optical flow techniques. IEEE 1992;0-81862855-3/92:236–42.
[15] Willert CE, Gharib M. Digital particle image velocimetry. Exp Fluids 1991;10:181–93.
[16] Lecompte D, Smits A, Sven Bossuyt, Sol H, Vantomme J, Van Hemelrijck D. Quality assessment of speckle patterns for digital image correlation. Opt Lasers Eng 2006;44:1132–45.
[17] Wang ZY, Li HQ, Tong JW, Ruan JT. Statistical analysis of the effect of intensity pattern noise on the displacement measurement precision of digital image correlation using self-correlated images; 2007. p. 701–7, doi:10.1007/s11340-006-9005-9.
[18] Scrivens WA, Luo Y, Sutton MA, Collete SA, Myrick ML, Miney P, et al. Development of patterns for digital image correlation measurements at reduced length scales. Exp Mech 2007;47:63–77.
[19] Muravsky LI, Sakharuk OM, Fityo NV, Yezhov PV. Increase the reliability of surface displacement field recovery by optical speckle-displacement correlation technique. Opt Lasers Eng 2007;45:993–1000.
[20] Jiang Zhenyu, Zhang Qingchuan, Jiang Huifeng, Chen Zhongjia, Wu Xiaoping. Spatial characteristics of the Portevin- Le Chatelier deformation bands in Al-4 at.%Cu polycrystals. Mater Sci Eng A 2005;403:154–64.
[21] Xiang GF, Zhang QC, Liu HW, Wu XP, Ju XY. Time-resolved deformation measures of the Portevin-Le Chatelier bands. Scr Mater 2007;56:721–4.
[22] Jiang Huifeng, Zhang Qingchuan, Jiang Zhenyu, Wu Xiaoping. Experimental investigations on kinetics of Portevin-Le Chatelier effect in Al-4 wt.% Cu alloys. J Alloys Compd 2007;428:151–6.
[23] Zhao Z, Ramesh M, Raabe D, Cuitiño AM, Radovitzky R. Investigation of three dimensional aspects of grain-scale plastic surface deformation of an aluminum oligocrystal. Int J Plasticity 2008;24:2278–97.
[24] Sánchez FM, Pulos G. Micro and macromechanical study of stress-induced martensitic transformation in a Cu–Al–Be polycrystalline shape memory alloy. Mat Sci Forum 2006;509:87–92.
[25] Sánchez-Arévalo F.M. 2007. "Estudio experimental del comportamiento mecánico de un material con memoria de forma" Ph. D. Thesis. Universidad Nacional Autónoma de México. México, 116 p.
[26] Chu TC, Ranson WF, Sutton MA, Peters WH. Aplications of digital correlation techniques to experimental mechanics. Exp Mech 1985;25(3):232–44.
[27] Kaouache B, Inal K, Bervellier S, Eberhardt A, Patoor E. Martensitic transformation criteria in Cu–Al–Be shape

memory alloy—in situ analysis. Mater Sci Eng A 2006;438–440:773–8.
[28] Yang JH, Wayman CM. Self-accommodation and shape memory mechanism of ε-Martensite I. Experimetal observations. Mater Charact 1992;28:23–35.
[29] Yang JH, Wayman CM. Self-accommodation and shape memory mechanism of ε-Martensite II. Theoretical considerations. Mater Charact 1992;28:37–47.
[30] Olson M, Cohen GB, Clapp PC. On the classification of displacement phase transformations. Proceedings of the international conference on martensitic transformation. ICOMAT 79; 1979. p. 1–11.